Ore Geology Reviews 86 (2017) 537–547

Contents lists available at ScienceDirect

Ore Geology Reviews

journal homepage: www.elsevier.com/locate/oregeo

Precambrian gold mineralization at Djamgyr in the Kyrgyz Tien Shan: Tectonic and metallogenic implications

D. Konopelko [a, b,*], R. Klemd [c], S.V. Petrov [a], F. Apayarov [d], B. Nazaraliev [e], O. Vokueva [f], A. Scherstén [f], S. Sergeev [a]

[a] St. Petersburg State University, 7/9 University Embankment, St., Petersburg 199034, Russia
[b] Novosibirsk State University, Pirogova St. 1, Novosibirsk, 630090, Russia
[c] GeoZentrum Nordbayern, Universität Erlangen-Nürnberg, Schlossgarten 5a, 91054 Erlangen, Germany
[d] North-Kyrgyz Geological Expedition, Ivanovka 725008, Kyrgyzstan
[e] OcOO Vertex-Gold Company, 2/4 Abaya St., Bishkek, Kyrgyzstan
[f] Department of Geology, Lund University, Sölvegatan 12, S-223 62 Lund, Sweden

ARTICLE INFO

Article history:
Received 7 December 2016
Received in revised form 2 March 2017
Accepted 3 March 2017 Available online 9 March 2017

Keywords:
Tien Shan (Tian Shan)
Talas-Fergana fault
Djamgyr (Jamgyr) Au deposit
Neoproterozoic

ABSTRACT

The Djamgyr gold deposit is located within the Neoproterozoic basement of the Middle Tien Shan terrane immediately west of the Talas-Fergana fault. The deposit comprises a system of auriferous quartz veins cross-cutting the Beshtor plagiogranite. The veins are surrounded by hydrothermal alteration aureoles and are oriented parallel to the Talas-Fergana fault. The Beshtor granite sampled in the vicinity of the deposit yielded a Neoproterozoic (Tonian) U-Pb zircon age of 815 ± 6 Ma, which is the first single grain zircon age of the Middle Tien Shan basement west of the Talas-Fergana fault. Ar-Ar dating of two mus-covite fractions from the alteration aureoles of the auriferous quartz veins yielded ages of 804 ± 3 and 805 ± 3 Ma suggesting that the mineralization in the Djamgyr deposit occurred during the Neoproterozoic ca. 10 m.y. after emplacement of the Beshtor granite. The structural pattern of the aurif-erous quartz veins and the new geochronological data, combined with the results of previous structural studies, may tentatively constrain the age of pre-existing major fault possibly marking an inherited ter-rane boundary in the northern part of the present-day Talas-Fergana strike-slip fault. The discovery of Precambrian gold mineralization in the Middle Tien Shan suggests re-evaluation of the metallogenic potential of its Precambrian basement that occupies significant areas west and east of the Talas-Fergana fault.

1. Introduction

The Tien Shan orogenic belt, stretching from the western deserts of Uzbekistan to the eastern Xinjiang in China for more than 2000 km, is known for its world-class ore deposits making this region the richest gold province of Eurasia. The majority of ore deposits in the Kyrgyz Tien Shan have formed during the late Paleozoic (Hercynian) evolution and final closure of the Turkestan (or Paleotethys) Ocean (e.g., Yakubchuk et al., 2002; Djenchuraeva, 2010). However, the implementation of advanced geochronological methods revealed older ages for several deposits, which increased the metallogenic potential of terranes that formed prior to middle Paleozoic times (e.g., Yakubchuk et al., 2010; Konopelko et al., 2014). Although Precambrian, mostly Neoproterozoic, blocks occupy significant parts of the Tien Shan (see Kröner et al., 2013 for review), gold mineralization in the Precambrian rocks is usually interpreted to be of late Paleozoic origin, while geochronologically constrained Precambrian gold deposits have not been reported in the whole belt until now (Rui et al., 2002; Nikonorov et al., 2007; Djenchuraeva, 2010; Goldfarb et al., 2014).

The Djamgyr gold deposit is located within a large Neoproterozoic block in the Kyrgyz Tien Shan and comprises a system of auriferous quartz veins, which occur parallel to the regional scale Talas-Fergana strike-slip fault that was active since the late Permian (cf. Rolland et al., 2013). Our sampling and investigation of the deposit area was aimed to constrain the timing of motions along the fault and its metallogenic potential. However, the obtained results of Ar-Ar and U-Pb dating revealed a Neoproterozoic age of the hydrothermal alteration and thus gold mineralization of the Djamgyr deposit. Below we describe the discovery of the first Precambrian gold deposit in the Kyrgyz Tien Shan and discuss the metallogenic and tectonic implications on a regional scale.

* Corresponding author at: Geological Faculty, St. Petersburg State University, 7/9 University Embankment, St., Petersburg 199034, Russia.
E-mail addresses: konopelko@inbox.ru, d.konopelko@spbu.ru (D. Konopelko).

http://dx.doi.org/10.1016/j.oregeorev.2017.03.007 0169-1368/

2. Principal terranes of the Kyrgyz Tien Shan and geological setting of the Djamgyr gold deposit

The Tien Shan orogenic belt formed during the late Paleozoic collisions between the Precambrian microcontinents of Karakum and Tarim in the south and the early Paleozoic Kazakhstan continent in the north (Zonenshain et al., 1990; Şengör et al., 1993; Windley et al., 2007; Biske and Seltmann, 2010; Biske et al., 2013; Burtman, 2015). The western Tien Shan in Kyrgyzstan is composed of three tectonic units (Fig. 1): (1) the Northern Tien Shan, the deformed margin of the Paleo-Kazakhstan continent; (2) the Middle Tien Shan, a middle to late Paleozoic continental arc developed at the southern margin of the Paleo-Kazakhstan; and (3) the Southern Tien Shan, a fold and thrust belt of tectonically superimposed Paleozoic passive margin and accretionary wedge units formed during the final closure of the Turkestan Ocean (Zonenshain et al., 1990; Biske and Seltmann, 2010; Burtman, 2015). Several major EW trending faults divide the Tien Shan into a series of linear terranes. These terranes are crosscut by the NW trending Talas-Fergana fault, which demonstrates a total dextral offset of about 200 km and separates the western Tien Shan terranes from the eastern terranes (Fig. 1).

The Northern Tien Shan in Kyrgyzstan and southernmost Kazakhstan is represented by the early Paleozoic continental magmatic arc built up on Precambrian basement. The arc formed as a result of subduction to the north with subsequent closure of the Terskey Ocean and accretion of the Middle Tien Shan to the Northern Tien Shan in the middle Ordovician (Lomize et al., 1997; Ghes, 2008; Degtyarev et al., 2017). East of the Talas-Fergana fault, the Northern and Middle Tien Shan terranes are separated by the Nikolaev Line, a late Paleozoic sinistral strike–slip fault generally following an early Paleozoic suture. The Talas-Karatau terrane of the Northern Tien Shan located on the NE wall of the Talas-Fergana fault (Fig. 1) represents a fragment of the Neoproterozoic – to early Paleozoic passive margin that is less affected by the early Paleozoic collisional events compared to other parts of the Northern Tien Shan (Maksumova et al., 2001).

Prior to accretion to the Northern Tien Shan, the Middle Tien Shan terrane developed as a southern passive margin of the Terskey Ocean (Ghes, 2008). A general feature of the Middle Tien Shan is a lack of early Paleozoic granitoids. To the west of the Talas-Fergana fault, the Neoproterozoic basement of the Middle Tien Shan is overlain by the latest Neoproterozoic clastic sediments that change upwards into Vendian diamictites and early Paleozoic shales, carbonates, cherts and turbidites (Osmonbetov and Knauf, 1982). Similar geological structures point to possible tectonic links between the Talas–Karatau terrane, the Middle Tien Shan, and the Tarim during the Neoproterozoic to early Paleozoic (Eganov and Sovetov, 1979). The Chatkal-Kurama volcano-plutonic belt, occupying a significant portion of the Middle Tien Shan, formed in a continental arc setting when the southern part of the Paleo-Kazakhstan continent developed as a northern active margin of the Turkestan Ocean during the middle and late Paleozoic (Fig. 1; Yakubchuk et al., 2002; Burtman, 2015). Final closure of the Turkestan Ocean in the late Carboniferous (e.g., Mühlberg et al., 2016) formed the Turkestan and Atbashi-Inylchek sutures separating the Middle and Southern Tien Shan terranes.

Major ore deposits of the Northern Tien Shan in western Kyrgyzstan are related to early and middle Paleozoic magmatism and include Cu-Au-Mo porphyry-type deposits, skarns and low sulfide Au deposits. The Middle Tien Shan west of the Talas-Fergana fault is known for its world-class Cu-Au-Mo porphyry-type deposits, skarns and epithermal Au deposits associated with suprasubduction Carboniferous and post-collisional early Permian magmatic pulses which formed the Chatkal-Kurama volcano-plutonic belt (Yakubchuk et al., 2002; Nikonorov et al., 2007; Djenchuraeva, 2010).

The Djamgyr gold deposit, which is hosted by the Neoproterozoic basement rocks of the Middle Tien Shan and juxtaposed to the Talas-Karatau terrane of the Northern Tien Shan, occurs almost immediately SW of the Talas-Fergana fault zone (Figs. 1 and 2). Auriferous quartz veins similar to those at the Djamgyr deposit comprise the Korumtor deposit and a number of occurrences in Kyrgyzstan and the adjacent territory of Uzbekistan (Nikonorov et al., 2007; Dunin-Barkovskaya and Koloskova, 2012).

3. Geology of the Djamgyr deposit area and previous geochronological studies

The Djamgyr gold deposit is located in the Talas range 2 km WSW of the Karabura mountain pass and ca. 1.5 km SW from the Talas-Fergana fault (Fig. 2). The area around the deposit is mapped at scales of 1:50,000 and 1:25,000 (Seliverstov and Datov, 1987; Shubin et al., 1992). The Neoproterozoic and early Paleozoic rocks in the deposit area are strongly deformed and metamorphosed under greenschist-facies conditions within a wide zone along the Talas-Fergana fault. On the NE wall of the Talas-Fergana fault, clastic metasediments of the Mesoproterozoic (middle Riphean) Karabura and Uzunakhmat Formations in the Talas–Karatau terrane are deformed in tight and subisoclinal folds parallel to the fault, overturned to the NE and cut by top-to-NE thrusts (Shubin et al., 1992; Rolland et al., 2013). On the SW wall of the Talas-Fergana fault, in the Middle Tien Shan terrane, deformed granites are dominant while minor metasediments are represented by siltstones and sandstones with subordinate volcaniclastics, cherts, carbonates and schists of the Korumtor, Ayaterek, Yaisamtor and Chakmak

Fig. 1. Principal tectonic zones and lineaments of the Tien Shan in Kyrgyzstan. Abbreviations: *NTS* – Northern Tien Shan, *MTS* – Middle Tien Shan, *STS* – Southern Tien Shan. Cross-hatched area shows outcrops of Precambrian basement, after Degtyarev et al. (2017), modified by the authors.

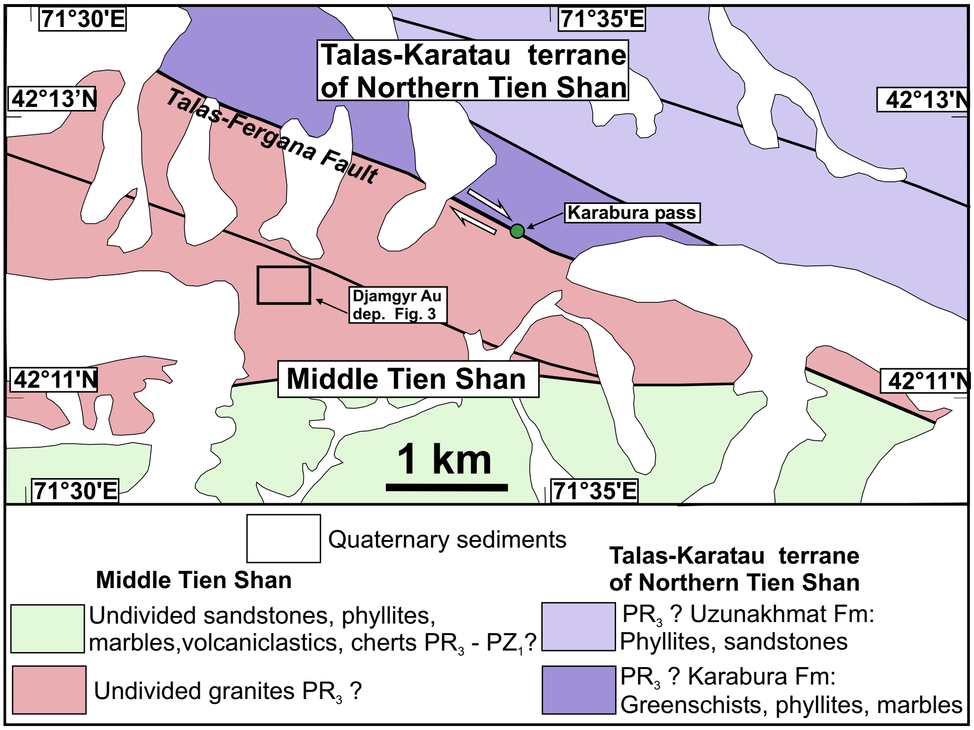

Fig. 2. Schematic geological map of the Djamgyr deposit area. After Shubin et al. (1992), modified by the authors.

Formations of inferred Neoproterozoic (late Riphean) to early Cambrian ages (Osmonbetov and Knauf, 1982; Shubin et al., 1992). In the field the Talas-Fergana fault occurs as a thick (up to 0.5 km) subvertical zone of variably mylonitized rocks with numerous tectonic slices of various ages striking in the area of the deposit roughly at 290° WNW.

A Precambrian age of the Middle Tien Shan basement was recognized in the early works of Sinitsin (1937), Zubtsov and Zubtsova (1963), Makarychev and Pavlova (1967) and other authors. In the last decades, ages in the range from 900 to 720 Ma were obtained for granites and felsic volcanics comprising the basement (Kiselev et al., 1993; Kröner et al., 2011, 2012; Konopelko et al., 2013). The granites in the vicinity of the deposit in the Middle Tien Shan terrane are represented by rose-grey porphyritic granites of the Muzbel massif of the Beshtor complex and by red granites of the Almasay complex (Osmonbetov and Knauf, 1982). Plagiogranites of the Beshtor intrusion, a type-locality of the Beshtor complex, were dated in the adjacent territory of Uzbekistan and yielded K-Ar ages in the range of 915 to 824 Ma (Ahmedov, 2000) and a multigrain U-Pb zircon age of 859 ± 22 Ma (Rafikov and Musaev, 1995). The granites of the Almasay complex are shown on geological maps as late Carboniferous based on a K-Ar biotite age of 285 Ma (Osmonbetov and Knauf, 1982). The geochronologically investigated rocks from both complexes occur far outside the Djamgyr deposit area.

In the Kyrgyz territory, the Djamgyr-type gold mineralization was considered as related to intrusions of the late Carboniferous or early Permian granites (Nikonorov et al., 2007; Djenchuraeva, 2010). This point of view was reflected on geological maps where auriferous quartz veins were shown as crosscutting both the Neoproterozoic and the late Carboniferous granites (e.g. Seliverstov and Datov, 1987; Shubin et al., 1992). The nearest largest example of the Djamgyr-type gold mineralization, the Korumtor gold deposit, is located ca. 8 km NW from the Djamgyr deposit along the Talas-Fergana fault. Auriferous quartz veins in the Korumtor deposit cut Neoproterozoic sediments, which were interpreted as a roof pendant of the late Carboniferous intrusion (Djenchuraeva, 2010). However, auriferous quartz veins in the Beshtor intrusion at the Tuyuk-Levoberezhny gold occurrence in the adjacent territory of Uzbekistan were tentatively interpreted to be similar in age to the surrounding Neoproterozoic plagiogranites (Dunin-Barkovskaya and Koloskova, 2012; Dunin-Barkovskaya et al., 2012).

4. Description of the Djamgyr gold deposit and sampling

The Djamgyr deposit was discovered in the 1980s by Seliverstov and Datov (1987). It is located on the SW slope of the Talas range at the altitudes of 3200–3600 m a. s. l. (Figs. 3, 4, and 5a). The territory of the deposit is mapped at scales of 1:5000 and 1:2000 (Sarbagishev and Nazaraliev, 2013). The dominant rock type in the deposit is represented by the Beshtor plagiogranite that is crosscut by a number of quartz veins generally striking NW along the Talas-Fergana fault (Fig. 3). The thickness of the quartz veins varies from a few cm to ca. 1 m. Individual small veins may comprise a series of parallel veins with a thickness of up to 5 m. According to Nikonorov et al. (2007), the gold mineralization is associated with quartz veins localized within two NW striking ore-bodies. Hydrothermal alteration aureoles in the host rocks around individual veins and vein swarms (0.1–10 m wide) are characterized by quartz, carbonate, muscovite and sericite, and K-feldspar assemblages, typical for orogenic gold-lode deposits (e.g., Goldfarb et al., 2001). The ore-body No 1 is 740 m long and 0.6–2 m wide, and the ore-body No 2 is 540 m long and 0.4–4 m wide (Figs. 3 and 4). As uncovered by drilling and mining, the auriferous quartz veins, comprising the two ore-bodies, form a relatively regular system of parallel veins steeply dipping to the NE (Figs. 4 and 5a). About 95% of the gold is represented by native gold disseminated in quartz, while the rest occurs as inclusions in sul-

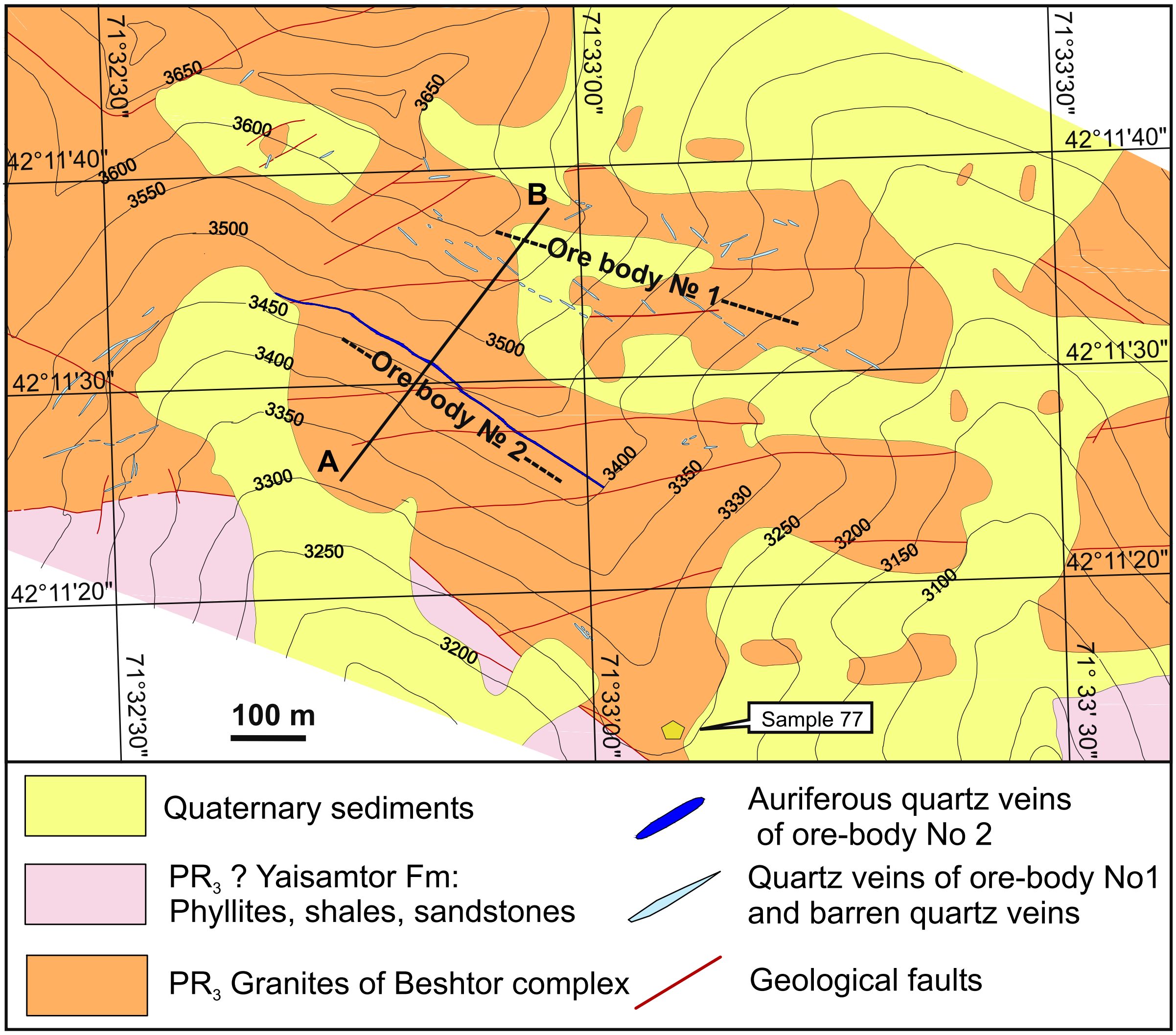

Fig. 3. Detailed geological map of the Djamgyr gold deposit. Based on Sarbagishev and Nazaraliev (2013), modified by the authors.

phides such as pyrite, chalcopyrite, arsenopyrite, galena, molybdenite and tennantite-tetrahedrite (Nikonorov et al., 2007). Channel sampling shows a very irregular distribution of gold in the quartz veins (Fig. 4). Native silver is also reported in the ores. The ores can be easily treated by a gravitation-cyanidation scheme with gold recovery of 98.4% (Nikonorov et al., 2007). The Soviet-style ore resources of C_2 category in the two ore-bodies, estimated by Shubin et al. (1992), included 5.336 tonnes of Au, grading 12.25 g/t Au. In addition, there are ca. 6 tonnes of Ag, grading 38.56 g/t and ca. 20,000 tonnes of Mo, grading 0.14%. The pre-mining resources of C_1 category of the ore-body No 2 were estimated in 2004 by Vertex-Gold Company OcOO at 0.535 tonnes of Au grading 17.72 g/t (Nikonorov et al., 2007; Nikonorov, 2009). The deposit is mined by Vertex-Gold Company since 2009. According to the “Fergana” News Agency, ca. 562 kg of Au was produced during 2009–2013 (Ivashchenko, 2013).

In order to estimate an age of the gold mineralization, several wall-rock samples of hydrothermal alteration aureoles around auriferous quartz veins were collected for the detailed petrographic study and subsequent A-Ar dating of the hydrothermal micas (Fig. 5c and d). The hydrothermally altered samples from the ore-body No 2 were collected by us from the ore storage and represent material obtained for processing. Sample 77, which was used for U-Pb zircon dating, was collected from a less altered host granite, ca. 450 m SSE from the ore-body No 2 at the lower levels of the deposit at the surface (Fig. 3).

5. Methodology and results

The methodology includes a petrographic description of the rock samples, U–Pb zircon geochronology of the granite surrounding the deposit, and Ar–Ar dating of muscovite concentrates from the ore samples. Mineral concentrates were produced at St. Petersburg State University. U-Pb zircon dating was performed in the VSEGEI, St. Petersburg, Russia, and the muscovite concentrates were dated in Lund University, Sweden. The results are presented in Tables 1 and 2 and Figs. 5–8.

5.1. Petrographic description of sampled rock-types

The granite hosting the deposit (Sample 77) is a medium-grained plagiogranite, consisting mainly of plagioclase and quartz as well as minor microcline-perthite. The rock is strongly brecciated and shows recrystallization of quartz surrounding granoblastic grains of plagioclase and growth of sericite along fractures (Fig. 5e). A strong limonitic and/or hematitic overprint is locally characteristic for the granite in the area close to the sampling site of Sample 77. Samples of the hydrothermal alteration, enveloping auriferous

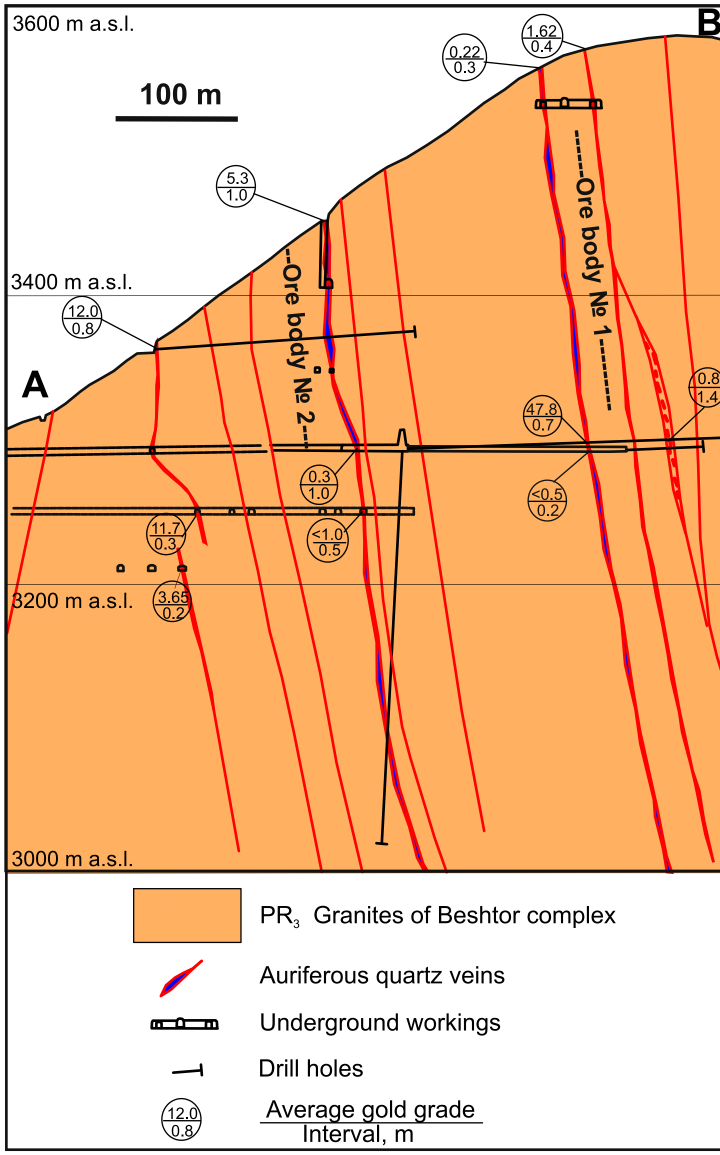

Fig. 4. Geological cross-section of the Djamgyr gold deposit. Based on Sarbagishev and Nazaraliev (2013), modified by the authors.

quartz veins (Fig. 5c and d), comprise strongly altered granite characterised by the pervasive growth of new muscovite and sericite, carbonate and quartz (Fig. 5f). Plagioclase is frequently sericitized, and biotite is altered to chlorite. The quartz shows strong dynamic recrystallization, and the secondary muscovite blades are often kinked and bent, indicating syntectonic deformation under greenschist-facies conditions (e.g., Lloyd, 1994). The rocks contain numerous mm-size fractures, formed as a result of brittle deformation, filled with a fine-grained aggregate of quartz, carbonate and sericite (Fig. 5g and h). In general, the described alteration patterns comprise typical mesothermal mineral assemblages (quartz + muscovite + carbonate ± chlorite ± pyrite ± arsenopyrite), characteristic of orogenic quartz vein gold deposits (e.g., Goldfarb et al., 2001; Marushchenko et al., 2015).

5.2. Zircon U–Pb age of the host granite

Selected zircon grains recovered from Sample 77 were hand-picked and mounted in epoxy resin together with chips of standard zircon grains. The grains were approximately sectioned in half and polished. Prior to analysis, zircon grains were investigated in transmitted and reflected light and under a scanning electron microscope equipped with cathodoluminescence (CL) detector. The U–Th–Pb isotope analyses were made using Sensitive High-Resolution Ion Microprobe (SHRIMP-II) in the Centre for Isotopic Research, VSEGEI, St. Petersburg, Russia. Each analysis consisted of four scans through the mass range. The diameter of the spot was about 30 μm, and the primary beam current was about 4 nA. Every fourth measurement was carried out on the zircon standard TEMORA 1, with an accepted $^{206}Pb/^{238}U$ age of 416.75 ± 0.24 Ma (Black et al., 2003). The Pb/U ratios have been normalized relative to a value of 0.0668 for the $^{206}Pb/^{238}U$ ratio of the TEMORA 1 standard. The zircon standard 91,500, with a U concentration of 81.2 ppm and an accepted $^{206}Pb/^{238}U$ age of 1065 Ma (Wiedenbeck et al., 1995) was used as a "U-concentration" standard. The data were reduced in a manner similar to that described by Williams (1998) and references therein, using the SQUID Excel Macro of Ludwig (2000). Corrections for common Pb were made using the ^{204}Pb isotope (measured $^{204}Pb/^{206}Pb$) and the present day terrestrial average Pb-isotopic composition (Stacey and Kramers, 1975). Uncertainties given for individual analyses in Table. 1 (ratios and ages) and Fig. 6 are at the 1σ level, however,

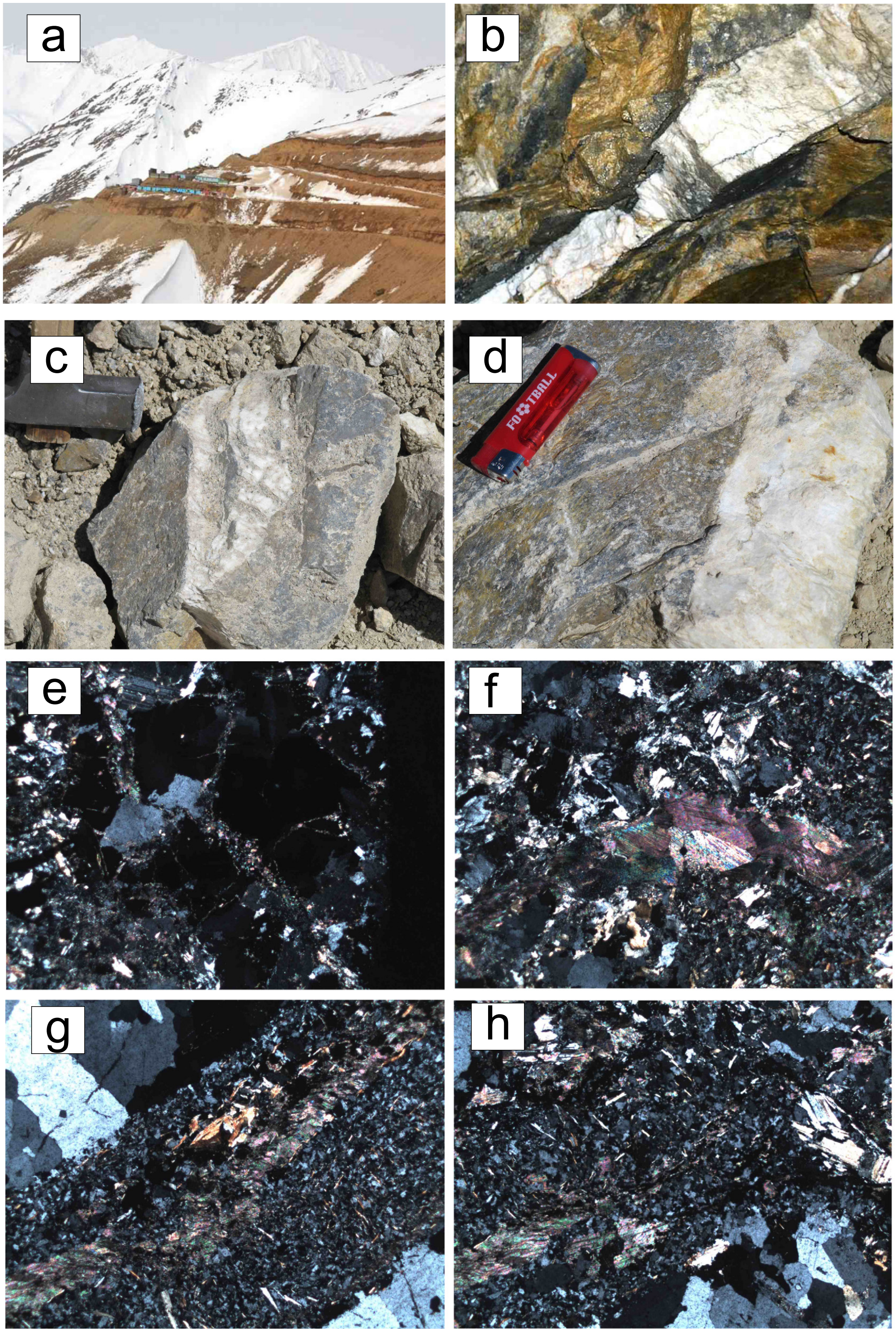

Fig. 5. (a) A view of the Djamgyr deposit from SE in wintertime. (b) Outcrop photograph of ca. 40 cm wide steeply dipping auriferous quartz vein in altered granite taken underground, ore-body No 2. (c and d) Hydrothermal alteration envelopes around auriferous quartz veins from ore-body No 2 sampled for Ar-Ar dating. (e and f) Photomicrographs of variably deformed and altered granites from alteration envelopes: (e) brecciated granite; (f) strongly altered brecciated granite with secondary sericite and carbonate. (g and h) Fractures, formed as a result of brittle deformation, filled with a fine grained aggregate of quartz, carbonate and sericite. Photographs a and b from Ivashchenko (2013).

Table 1
U-Pb analytical data and calculated ages.

Sample-spot #[a]	Concentrations					Isotope ratios[c]							Age (Ma)				
	U ppm	Th ppm	Th/U	$^{206}Pb^*$ ppm	f206[b] %	$^{207}Pb^*/^{206}Pb^*$	±1σ %	$^{207}Pb^*/^{235}U$	±1σ %	$^{206}Pb^*/^{238}U$	±1σ %	err.[d] corr.	$^{206}Pb^*/^{238}U$	±1σ	$^{207}Pb^*/^{206}Pb$	±1σ	Disc.[e] %
Sample 77 – granite (N 42° 11′14.0″, E 71° 33′03.8″)																	
77.7.1	218	169	0.80	25.0	0.24	0.0653	2.8	1.19	3.0	0.1326	1.1	.365	803	8	783	59	-2
77.5.1	239	218	0.94	27.3	0.47	0.0666	3.2	1.22	3.4	0.1327	1.1	.319	803	8	827	67	3
77.8.1	286	254	0.92	32.9	0.30	0.0666	2.8	1.22	2.9	0.1333	1.0	.350	807	8	826	58	2
77.4.1	226	125	0.57	26.0	0.18	0.0656	3.0	1.21	3.2	0.1336	1.1	.344	808	8	793	62	-2
77.3.1	243	201	0.86	28.3	0.05	0.0672	1.9	1.26	2.1	0.1356	1.1	.492	820	8	843	39	3
77.1.1	295	275	0.96	34.5	0.19	0.0662	2.1	1.24	2.4	0.1356	1.0	.424	820	8	812	45	-1
77.2.1	299	291	1.00	35.1	0.11	0.0670	1.9	1.26	2.1	0.1364	1.0	.468	824	8	839	39	2
77.6.1	314	338	1.11	36.9	0.18	0.0655	2.0	1.23	2.3	0.1365	1.0	.437	825	8	789	43	-4

[a] The last two digits denote number of grain and number of analytical spot within the grain.
[b] f206 denotes 100*(common ^{206}Pb)/(total measured ^{206}Pb).
[*] Radiogenic Pb.
[c] Corrected for ^{204}Pb.
[d] Error correlation $^{207}Pb/^{235}U$ – $^{206}Pb/^{238}U$.
[e] Disc. % denotes 100*((1 – (age$^{206}Pb/^{238}U$)/(age$^{207}Pb/^{206}Pb$)).

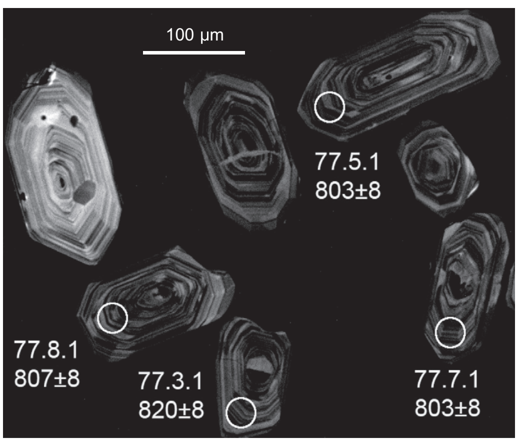

Fig. 6. CL images of analyzed zircon grains from granite Sample 77. Ovals define analytical spots. Sample and spot numbers are as in Table 1 Ages are in Ma, errors at 1σ level.

the uncertainties in calculated concordia ages (Fig. 7) are reported at 2σ level. The concordia plots were constructed using the ISOPLOT/EX macro (Ludwig, 1999).

The plagiogranite Sample 77 produced a datable population of stubby prismatic zircon grains with well-shaped facets and pronounced oscillatory zoning (Fig. 6). Eight zircon domains in 8 grains were analyzed. The analyzed zircon domains have U and Th contents in the range of 169–338 ppm and relatively high Th/U ratios >0.2 (0.57–1.11, Table. 1), typical for magmatic zircon (Kirkland et al., 2015 and references therein). Analytical data for Sample 77 are concordant and plot as tight clusters, for which a $^{206}Pb/^{238}U$ concordia age of 815 ± 6 Ma was calculated (Fig. 7), which is considered as a good estimate of a crystallization age of the Beshtor plagiogranite.

5.3. $^{40}Ar/^{39}Ar$ analysis of muscovite concentrates

Muscovite crystals recovered from the alteration aureoles (Samples 78 and 79) were pre-treated to remove possible traces of

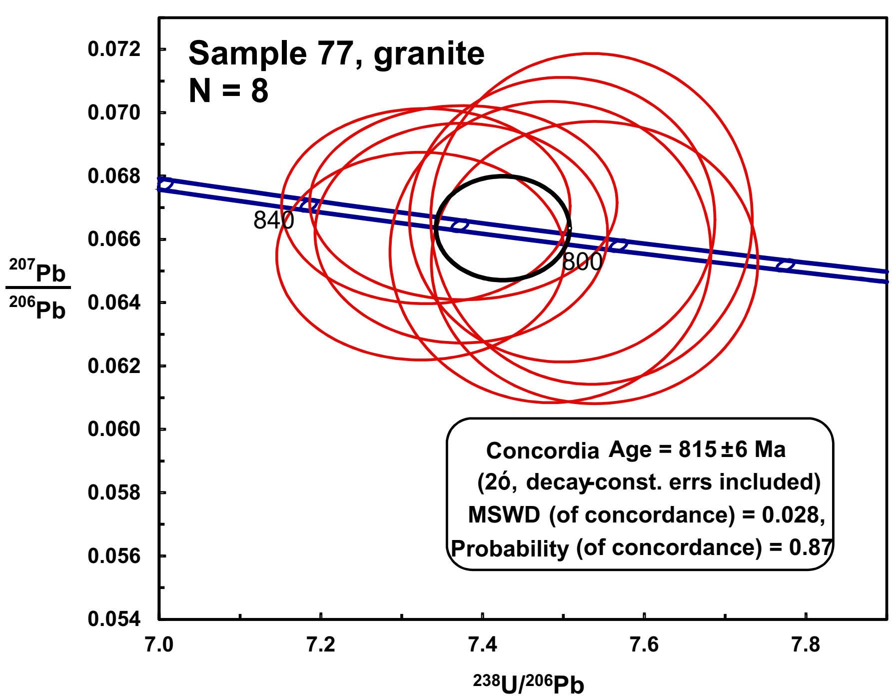

Fig. 7. Concordia diagram for zircon U–Pb SHRIMP data of granite Sample 77. Sample numbers as in Table 1.

Table 2
Results of $^{40}Ar/^{39}Ar$ analysis of muscovite concentrates.

Sample	Plateau age				
	N/N^{tot}	Age	±2σ (Ma)	^{39}Ar (%)	MSWD
78	6/13	804	3	69.9	0.92
79	10/16	805	3	43.6	2.47

Given are number of increments included in the age calculation, % of ^{39}Ar released from the sample and included in the age calculation and Mean Square Weighted Deviation (MSWD) for plateau age calc.

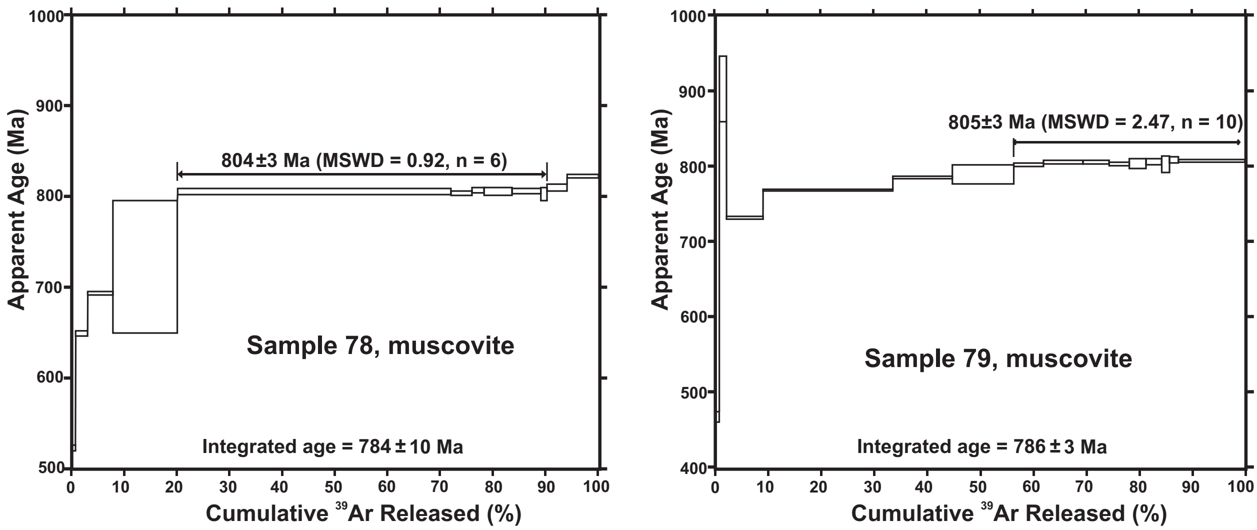

Fig. 8. $^{40}Ar/^{39}Ar$ step-heating spectra for Samples 78 and 79. Data and results at 2 sigma.

weathered material, separated by standard techniques and selected by handpicking under a binocular microscope from the 50–200 μm size fraction. Argon was measured from at least two different aliquots of the same concentrate. The Geochronology laboratory at the University of Lund uses a Micromass 5400 mass spectrometer with a Faraday and an electron multiplier. The sample, which was loaded into a copper planchette that contains several 3 mm holes, was step-heated using a defocused 50 W CO_2-laser. Rastering the laser beam over the sample provided uniform heating of all grains. An automated analytical process runs on a Macintosh OS 10.2 platform with software customized for the Lund laboratory. Regressions to time zero were fitted to data collected from ten scans over the mass range of 36 to 40. Peak heights and backgrounds were corrected for mass discrimination, isotope decay and interfering nucleogenic Ca-, K- and Cl-derived isotopes. Sanidine standard TCR (t = 28.34 Ma, Renne et al., 1998) was used, and J values were calibrated with a precision of ±0.25%. The samples were irradiated at the Petten reactor. A step-heating age spectrum plot displays a plateau age interpreted to be meaningful when the apparent age for at least three consecutive steps comprises a minimum of 50% of the total released ^{39}Ar (Dickin, 2005). ISOPLOT/EX macro (Ludwig, 1999) was used to calculate the ages and 2σ errors.

Both muscovite concentrates Sample 78 and 79 yielded relatively variable $^{40}Ar/^{39}Ar$ spectra with similar characteristics (Table. 2, Fig. 8). The intermediate and high-energy steps recorded a systematic increase of apparent ages. A well-defined plateau age of 804 ± 3 Ma (MSWD = 0.92), including 6 adjacent steps and 69.9% of the released ^{39}Ar, is assumed to be a good estimate of the geological age of the hydrothermal muscovite of Sample 78. A plateau age of 805 ± 3 Ma (MSWD = 2.47), including 10 adjacent steps and 43.6% of the released ^{39}Ar, obtained for Sample 79 is poorly defined but co-insides within error limits with an age obtained for Sample 78. Finally, integrated ages of 784 ± 10 and 786 ± 3 Ma, obtained for Samples 78 and 79, respectively, clearly show that formation of the hydrothermal alteration and the associated gold mineralization occurred in the Neoproterozoic (Tonian) and not in the late Paleozoic as was previously suggested (Nikonorov et al., 2007; Djenchuraeva, 2010). The new ages also demonstrate that the gold mineralization (assuming a simultaneous formation of the gold and associated hydrothermal alteration) occurred ca. 10 m.y. after the emplacement of the host-rock granite that yielded a U-Pb zircon age of 815 ± 6 Ma.

6. Discussion

6.1. Tectonic implications

6.1.1. Age of the Middle Tien Shan basement

Precambrian terranes constitute more than 50% of the western Tien Shan crust and form several relatively narrow and long blocks separated from each other by Paleozoic orogenic belts marked with ophiolites. Recent geochronological studies showed that some high-grade metamorphic terranes, previously interpreted as Archean to Paleoproterozoic basement, are much younger and consist of late Precambrian rock assemblages. The two major crust-forming events, recognized in the last decades, include 1.3–1.1 Ga Mesoproterozoic (Tarimian or Issedonian) and 950–700 Ma Neoproterozoic (Baikalian or Ulutau-Moyunkum) tectonic cycles (see Kröner et al., 2013; Konopelko and Klemd, 2016 and Degtyarev et al., 2017 for review). In the Kyrgyz Tien Shan, ages in the range of 1.3 to 1.1 Ga are characteristic for the Northern Tien Shan while ages in the range of 950–700 Ma were established in the Middle Tien Shan and in the Karatau-Talas terrane (Degtyarev et al., 2017 and references therein). In the Middle Tien

Shan, single grain zircon ages of 778 and 728 Ma were obtained for deformed granites located immediately NE of the Talas-Fergana fault ca. 200 km SE of the Djamgyr deposit (Konopelko et al., 2013), and ages of 836, 806 and 764 Ma were reported for felsic volcanics and granitoids outcropping several hundred kilometres east of the Talas-Fergana fault (Kröner et al., 2013 and references therein). Earlier, multigrain and discordant U–Pb zircon ages of 806 and 753 Ma were reported for granitoids from the Middle Tien Shan and Talas-Karatau terrane, respectively, sampled in the immediate vicinity of the Talas-Fergana fault ca. 150 km NW from the Djamgyr deposit in the territory of Kazakhstan (Kozakov, 1993). These ages are compatible with four maximum depositional ages in the range of 800 to 750 Ma, reported by Rojas-Agramonte et al. (2014) for clastic metasediments of the Talas-Karatau terrane in the territory of Kyrgyzstan, ca. 20 km NE of the Djamgyr deposit. Thus, an age of 815 ± 6 Ma, obtained in this study for the Beshtor plagiogranite, is in good agreement with published ages for the Middle Tien Shan basement and comprises the first single grain zircon age reported for the basement west of the Talas-Fergana fault. Further west the Middle Tien Shan basement is overlain by middle Paleozoic to Cenozoic sedimentary basins, with only limited exposure west of the Talas-Fergana fault. However, drilling and geophysical data suggested presence of buried terranes, such as the large Syrdaria block, occupying the entire area of the western deserts of Uzbekistan and Kazakhstan and possibly composed of similar Meso- to Neoproterozoic formations (Degtyarev et al., 2017 and references therein).

6.1.2. Possible age of the inherited terrane boundary in the northern part of Talas-Fergana fault

The Talas-Fergana fault strikes across the Tien Shan structures for ca. 1500 km from Kazakhstan to western Tarim. The dextral displacement along the fault from the early Permian to present time reached ca. 200 km in its central part based on the offset of the Turkestan and Atbashi-Inylchek sutures (Fig. 1). The main shear displacement along the fault occurred in the late Permian to Triassic. The amplitude of displacement decreases from the central part of the Talas-Fergana fault to its NW and SE terminations (Burtman, 2015 and references therein). Several researchers pointed out that the Talas-Fergana fault obviously inherited a pre-existing terrane boundary. Based on different tectonic scenarios of convergence and timing of collisional events to the west and to the east of the fault, Charvet et al. (2011) and Loury et al. (2015) proposed that during the Carboniferous the Tarim and Alai microcontinents were separated by a major transform fault that was later converted into an intra-continental strike-slip fault. Other authors (e.g. Şengör et al., 1993; Burtman, 2015) suggested that in its northern part the Talas-Fergana fault probably inherited an early Paleozoic terrane boundary as indicated by juxtaposition of two terranes (the Middle Tien Shan and the Talas-Karatau) that have different early Palaeozoic geological histories and are both overlain by similar Devonian redbeds. Voytenko and Khudoley (2012) showed that structural patterns of the ca. 70 km-long and 8 km-wide Usunakhmat unit of the Talas–Karatau terrane, bound to the Talas-Fergana fault in the area of the Djamgyr deposit, were formed prior or during the early Paleozoic. They suggested that during the late Paleozoic the fault was reactivated with displacement parallel to already formed folds and thrusts of the Usunakhmat unit, which explains why it does not show a cross-cutting relationship with the early Paleozoic structures. The geometry of deformations along the Talas-Fergana fault near Karabura pass in the immediate vicinity of the Djamgyr deposit was recently studied by Rolland et al. (2013) who showed that the granites to the SW of the fault are cross-cut by numerous ductile to brittle shear zones parallel to the fault and demonstrated combined dextral and top-to-the south motion. Based on brittle-ductile deformation

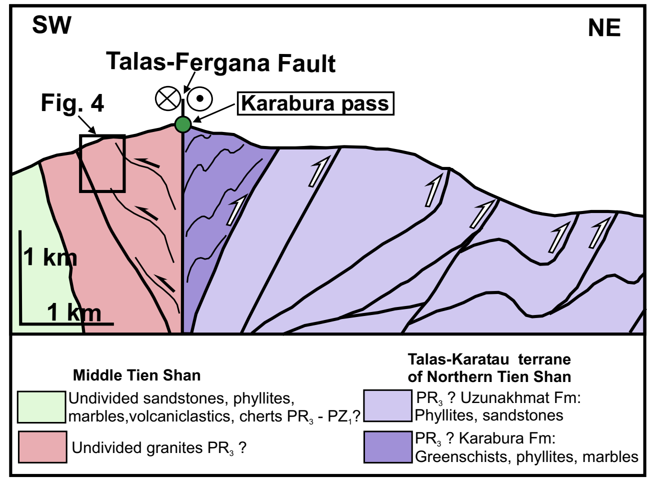

Fig. 9. A schematic geological transect across the Talas–Fergana fault near Karabura mountain pass, after Rolland et al. (2013), modified by the authors.

of quartz and brittle strain of K-feldspar, these authors concluded that the temperature conditions during shearing were close to 300 °C, i.e. under greenschist-facies conditions. The deformational patterns observed on both sides of the Talas-Fergana fault in the area of the Djamgyr deposit are in agreement with a positive flower structure that may have formed in a transpressive regime (Fig. 9) (Rolland et al., 2013).

The Djamgyr deposit is located ca. 1.5 km SW of the Talas-Fergana fault within the area studied by Rolland et al. (2013). Detailed geological cross-section (Fig. 4) clearly demonstrates that the orientation of the auriferous quartz veins at the Djamgyr deposit is parallel to that of the Talas-Fergana fault and perfectly matches their expected position in the described flower structure (Fig. 9) and may be explained by top-to-the south motions in a transpressive regime. However, our new ages indicate that ductile to brittle deformation of the surrounding granite, that controlled gold mineralization at the Djamgyr deposit, had already occurred as early as in the Neoproterozoic (Tonian), much earlier than it was previously thought (Nikonorov et al., 2007; Djenchuraeva, 2010). Consequently, the Neoproterozoic age established for the Djamgyr gold deposit may substantiate the former presence of a pre-existing major fault, possibly marking an inherited terrane boundary in the northern part of the present-day Talas-Fergana strike-slip fault.

6.2. Metallogenic implications

Available statistics on discovery of gold deposits show that during the last decade discovery rates of new deposits were declining and the cost per discovery was rising steeply, bringing the whole industry to a situation close to a zero return. This was explained by a tendency to study ore-forming processes at the deposit scale, despite employing a hierarchical approach from province through district to deposit scales (Groves, 2014). The situation can be improved by changing the nature of greenfields exploration by evaluating each exploration target in terms of its larger scale tectonic and temporal setting to assess its true potential.

A Neoproterozoic age obtained for the Djamgyr gold deposit represents an example when a deposit scale study allows re-evaluation of the metallogenic potential of a wider terrane. Previously, all gold deposits in the Tien Shan were considered to be Phanerozoic in age and the absence of Precambrian gold deposits was explained by the fact that exposed Precambrian rocks are of relatively high-metamorphic grade and define deeper crustal levels than those that would contain preserved Precambrian gold deposits (Nikonorov et al., 2007; Djenchuraeva, 2010; Goldfarb et al., 2014). However, our recent work has already shown that some Neoproterozoic terranes in the Kyrgyz Tien Shan may have metallogenic potential for ore deposits (Konopelko et al., 2014). The new discovery of a Precambrian gold deposit in the Middle Tien Shan suggests further re-assessment of the metallogenic potential of its Precambrian basement that occupies significant areas west and east of the Talas-Fergana fault (Fig. 1). However, the geodynamic setting of the Neoproterozoic gold occurrences in the Middle Tien Shan basement remains poorly constrained. The Yenisei Ridge region, a late Neoproterozoic orogenic belt along the SW margin of the Siberia craton, is perhaps the closest equivalent of the Middle Tien Shan terrane in the Central Asian Orogenic Belt with significant recognized gold resources formed in the late Neoproterozoic (Goldfarb et al., 2014). Both terranes probably represented independent blocks within the Paleotethys Ocean, subsequent to ca. 900–800 Ma rifting from their poorly constrained positions within the Rodinia supercontinent (Cocks and Torvsik, 2007; Yakubchuk, 2017). Thus, future exploration, focused on deciphering geodynamic settings of magmatic rocks in combination with structural studies, may potentially result in finding of new exploration targets in the Middle Tien Shan basement.

7. Conclusions

Here we report for the first time a Neoproterozoic (Tonian) single grain U-Pb zircon age of 815 ± 6 Ma for the Beshtor granite of the Middle Tien Shan basement west of the Talas-Fergana fault. Ar-Ar dating of two muscovite fractions from the hydrothermal alteration aureoles of the auriferous quartz veins of the Djamgyr gold deposit hosted by the Beshtor granite yielded ages of 804 ± 3 and 805 ± 3 Ma indicating that the hydrothermal alteration and thus the ore-formation in the Djamgyr deposit occurred during the Neoproterozoic, ca. 10 m.y. after the emplacement of the Beshtor granite. The structural pattern of the auriferous quartz veins and the new geochronological data, combined with the results of previous structural studies, may tentatively constrain the age of pre-existing major fault possibly marking an inherited terrane boundary in the northern part of the present-day Talas-Fergana strike-slip fault. The recognition of the Precambrian gold mineralization in the Middle Tien Shan suggests a re-assessment of the metallogenic potential of its Precambrian basement that occupies significant areas west and east of the Talas-Fergana fault.

Acknowledgements

We are grateful to Anatoly Ilyukhin who was responsible for logistics and transportation in the field. OcOO Vertex-Gold Company is acknowledged for access to the Djamgyr deposit. We appreciate constructive reviews of Jacques Charvet and Alexander Yakubchuk that helped to improve the first version of the manuscript. D. Konopelko was supported by the Ministry of Education and Science of the Russian Federation (project No 14.Y26.31.0018) and by research and field work grants 3.38.137.2014, 3.42.1501.2015 and 3.42.1107.2016 from Saint Petersburg State University.

References

Ahmedov, N.A. (Ed.), 2000. Stratified and Intrusive Formations of Uzbekistan. Tashkent, p. 511 (in Russian).

Biske, Yu.S., Seltmann, R., 2010. Paleozoic Tian-Shan as a transitional region between the Rheic and Urals-Turkestan Oceans. Gondwana Res. 17, 602–613.

Biske, Yu.S., Konopelko, D., Seltmann, R., 2013. Geodynamics of the Late Paleozoic magmatism of Tien Shan and surrounding territories. Geotectonics 47 (4), 291–309.

Black, L.P., Kamo, S.L., Allen, C.M., Aleinikoff, J.N., Davis, D.W., Korsch, R.J., Foudoulis, C., 2003. TEMORA 1: a new zircon standard for U-Pb geochronology. Chem. Geol. 200, 155–170.

Burtman, V.S., 2015. Tectonics and Geodynamics of the Tian Shan in the Middle and Late Paleozoic. Geotectonics 49 (4), 302–319.

Charvet, J., Shu, L., Laurent-Charvet, S., Wang, B., Faure, M., Cluzel, D., Chen, Y., Jong, K., 2011. Palaeozoic tectonic evolution of the Tianshan belt, NW China. Sci. China Earth Sci. 54, 166–184. http://dx.doi.org/10.1007/s11430-010-4138-1.

Cocks, L.R.M., Torvsik, T.H., 2007. Siberia, the wandering northern terrane, and its changing geography through the Paleozoic. Earth Sci. Rev. 82, 29–74.

Degtyarev, K., Yakubchuk, A., Tretyakov, A., Kotov, A., Kovach, V., 2017. Precambrian geology of the Kazakh uplands and Tien Shan: an overview. Gondwana Res. http://dx.doi.org/10.1016/j.gr.2016.12.014.

Dickin, A.P., 2005. Radiogenic Isotope Geology. Cambridge University Press, UK, p. 492.

Djenchuraeva, R.D., 2010. Geodynamics, Metallogeny and Ore Genesis (Tien Shan and Surrounding Territories). "Yilim" Publishing House, Bishkek, p. 211 (in Russian).

Dunin-Barkovskaya, E.A., Koloskova, S.M., 2012. Mineral and Geochemical Features of Gold Mineralization in the Beshtor-Tunduk massif of Proterozoic Plagiogranites and its Metallogenic Potential. Geol Miner. Resour. 2 (in Russian).

Dunin-Barkovskaya, E.A., Koloskova, S.M., Muhamedjanova, D.V., 2012. Paragenesis of gold and monazite in quartz veins of the Beshtor-Tunduk massif of Neoproterozoic plagiogranites. Proceedings of conference "Current Problems of Connections Between Geodynamics, Magmatism and Mineralization". "Fan" Publishing House of Academy of Sciences of Republic of Uzbekistan, Tashken, pp. 113–120 (in Russian).

Eganov, E.A., Sovetov, Yu.K., 1979. Karatau - A Model for Phosphorite Deposition. The Institute of Geology and Geophysics Ac. Sci USSR, Transactions, Issue 427. Novosibirsk "Nauka", 190 p. (in Russian).

Ghes, M.D., 2008. Terrane Structure and Geodynamic Evolution of the Caledonides of Tian-Shan. Altyn Tamga Publishing House, Bishkek, p. 158 (in Russian).

Goldfarb, R., Groves, D.I., Gardoll, S., 2001. Orogenic gold and geologic time: a global synthesis. Ore Geol. Rev. 18, 1–75.

Goldfarb, R.J., Taylor, R.D., Collins, G.S., Goryachev, N.A., Orlandini, O.F., 2014. Phanerozoic continental growth and gold metallogeny of Asia. Gondwana Res. 25, 48–102.

Groves, D.I., 2014. Importance of craton margins and other lithosphere boundaries for gold and other metal exploration. In: Convention &11th International Conference on Gondwana to Asia 20-21 September 2014, Beijing, China, Abstract Volume, IAGR Conference Series 20, 39–40.

Ivashchenko, E., 2013. Gold veins of Kyrgyzstan. International information agency "Fegrana", http://www.fergananews.com/articles/7693 (in Russian).

Kirkland, C.L., Smithies, R.H., Taylor, R.J.M., Evans, N., McDonald, B., 2015. Zircon Th/U ratios in magmatic environs. Lithos 212–215, 397–414.

Kiselev, V.V., Apayarov, F.Kh., Komartsev, V.T., Tsyganok, E.N., Lukashova, E.M., 1993. Isotopic ages of zircons from crystalline complexes of the Tianshan. In: Kozakov, I.K. (Ed.), Early Precambrian of the Central Asia Folded Belt. Nauka, Leningrad, pp. 99–115 (in Russian).

Konopelko, D., Seltmann, R., Apayarov, F., Belousova, E., Izokh, A., Lepekhina, E., 2013. U-Pb–Hf zircon study of two mylonitic granite complexes in the Talas-Fergana fault zone, Kyrgyzstan, and Ar–Ar age of deformations along the fault. J. Asian Earth Sci. 73, 334–346.

Konopelko, D., Biske, G., Seltmann, R., Petrov, S.V., Lepekhina, E., 2014. Age and petrogenesis of the Neoproterozoic Chon-Ashu alkaline complex, and a new discovery of chalcopyrite mineralization in the eastern Kyrgyz Tien Shan. Ore Geol. Rev. 61, 175–191.

Konopelko, D., Klemd, R., 2016. Deciphering protoliths of the (U)HP rocks in the Makbal metamorphic complex, Kyrgyzstan: geochemistry and SHRIMP zircon geochronology. Eur. J. Mineral. 28 (6), 1233–1253. http://dx.doi.org/10.1127/ejm/2016/0028-2602.

Kozakov, I.K. (Ed.), 1993. The early Precambrian of the Central Asia Fold Belt. Nauka, St. Petersburg, p. 272 (in Russian).

Kröner, A., Alexeiev, D.V., Rojas-Agramonte, Y., Wong, J., Mikolaichuk, A., Kiselev, V. V., Liu, D., Sun, M., 2011. New single zircon ages and Hf isotopic systematics for igneous and metamorphic rocks of the Kyrgyz Tianshan and tectonic implications. In: Abstracts, Fifth International Symposium: Modern Problems of Geodynamics and Geoecology of Intracontinental Orogens, Bishkek, 19–24, June 2011, vol. 2, 207–208.

Kröner, A., Alexeiev, D.V., Hegner, E., Rojas-Agramonte, Y., Corsini, M., Chao, Y., Wong, J., Windley, B.F., Liu, D., Tretyakov, A.A., 2012. Zircon and muscovite ages, geochemistry, and Nd–Hf isotopes for the Aktyuz metamorphic terrane: evidence for an Early Ordovician collisional belt in the northern Tianshan of Kyrgyzstan. Gondwana Res. 21, 901–927.

Kröner, A., Alexeiev, D.V., Rojas-Agramonte, Y., Hegner, E., Wong, J., Xia, X., Belousova, E., Mikolaichuk, A., Seltmann, R., Liu, D., Kisilev, V., 2013. Mesoproterozoic (Grenville-age) terranes in the Kyrgyz North Tianshan: Zircon ages and Nd-Hf isotopic constraints on the origin and evolution of basement blocks in the southern Central Asian Orogen. Gondwana Res. 23, 272–295.

Lloyd, G.R., 1994. Dynamic recrystallization of quartz under greenschist conditions. J. Struct. Geol. 16, 867–881.

Lomize, M.G., Demina, L.I., Zarshchikov, A.A., 1997. The Kyrgyz-Terskei Paleo-oceanic Basin, Tien Shan. Geodynamics 6, 35–55.

Loury, C., Rolland, Y., Cenki-Tok, B., Lanari, P., Guillot, S., 2015. Late Paleozoic evolution of the South Tien Shan: Insights from P-T estimates and allanite

geochronology on retrogressed eclogites (Chatkal range, Kyrgyzstan). J. Geodyn. http://dx.doi.org/10.1016/j.jog.2015.06.005.
Ludwig, K.R., 1999. User's manual for Isoplot/Ex, Version 2.10, A geochronological toolkit for Microsoft Excel. Berkeley Geochronology Center Special Publication No 1a, 2455 Ridge Road, Berkeley CA 94709, USA.
Ludwig, K.R., 2000. SQUID 1.00, A User's Manual; Berkeley Geochronology Center Special Publication. No 2, 2455 Ridge Road, Berkeley, CA 94709, USA.
Makarychev, G.I., Pavlova, T.G., 1967. Riphean of the western part of the Middle Tien Shan. MOIP Bull. 42–1, 5–19 (in Russian).
Maksumova, R.A., Dzhenchuraeva, A.V., Berezanskiy, A.V., 2001. Structure and evolution of the Tien Shan nappe-folded orogen. Russ. Geol. Geophys. 42, 1367–1374.
Marushchenko, L.I., Baksheev, I.A., Nagornaya, E.V., Chitalin, A.F., Nikolaev, Yu.N., Kal'ko, I.A., Prokofiev, V.Yu., 2015. Quartz–sericite and argillic alterations at the Peschanka Cu–Mo–Au deposit, Chukchi Peninsula, Russia. Geol. Ore Deposits 57–3, 213–225.
Mühlberg, M., Hegner, E., Klemd, R., Pfänder, J.A., Kaliwoda, M., Biske, Y.S., 2016. Late Carboniferous high-pressure metamorphism of the Kassan Metamorphic Complex (Kyrgyz Tianshan) and assembly of the SW Central Asian Orogenic Belt. Lithos 264, 41–55.
Nikonorov, V.V., Karaev, Yu.V., Borisov, F.I., Tolsky, V.I., Zamaletdinov, T.S., Larina, T. V., Gorbaneva, T.V., 2007. Gold Resources of Kyrgyzstan. State Agency for Geology and Mineral Resources, Bishkek, p. 500.
Nikonorov, V.V., 2009. Ore Deposits of Kyrgyzstan. Bishkek, p. 482 (in Russian).
Osmonbetov, K.O., Knauf, V.I. (Eds.), 1982. Stratified and Intrusive Formations of Kyrgyzia, vols. 1 and 2. Yilim" Publishing House, Frunze, Kyrgyz SSR (in Russian).
Rafikov, Ya.M., Musaev, A.A., 1995. Geochronology of intrusive complexes of the Chatkal zone: - new data of U-Pb, Rb-Sr, and K-Ar methods. Uzbek Geol. J. 2, 29–35 (in Russian).
Renne, P.R., Swisher, C.C., Deino, A.L., Karner, D.B., Owens, T.L., DePaolo, D.J., 1998. Intercalibrations of standards, absolute ages and uncertainties in 40Ar/39Ar dating. Chem. Geol. 145, 117–152.
Rojas-Agramonte, Y., Kröner, A., Alexeiev, D.V., Jeffreys, T., Khudoley, A.K., Wong, J., Geng, H., Shug, L., Semiletkin, S.A., Mikolaichuk, A.V., Kiselev, V.V., Yang, J., Seltmann, R., 2014. Detrital and igneous zircon ages for supracrustal rocks of the Kyrgyz Tianshan and palaeogeographic implications. Gondwana Res. 26, 957–974.
Rolland, Y., Alexeiev, D.V., Kröner, A., Corsini, M., Loury, C., Monié, P., 2013. Late Palaeozoic to Mesozoic kinematic history of Talas-Ferghana strikeslip Fault (Kyrgyz West Tianshan) revealed by a structural study and $^{40}Ar/^{39}Ar$ dating. J. Asian Earth Sci. 67–68, 76–92.
Rui, Z., Goldfarb, R., Qiu, Y.M., Zhou, T., Chen, R., Pirajno, F., Yun, G., 2002. Paleozoic–early Mesozoic gold deposits of the Xinjiang Autonomous Region, northwestern China. Miner Deposita 37, 393–418.
Sarbagishev, N.R., Nazaraliev, B.A., 2013. Technical report including pre-mining resource calculations for ore-body No 2 of the Djamgyr deposit with feasibility study. (Unpublished, in Russian).
Seliverstov, K.V., Datov, R.P. et al., 1987. Technical report "Otchet Sandalashskoy partii o resultatah poiskovikh rabot v Sandalashskom rudnom raione I poiskovo-otsenochnikh rabot na Kichisandikskom i Turpaktushtinskom rudnokh polyakh, provedennikh v 1980-1987 gg". Chatkalskaya geologicheskaya expeditsiya. Frunze (Bishkek), Geological library of the State Agency for Geology and Mineral Resources (unpublished, in Russian).
Şengör, A.M.C., Natal'in, B.A., Burtman, V.S., 1993. Evolution of the Altaid tectonic collage and Paleozoic crust growth in Eurasia. Nature 364, 299–307.
Sinitsin, N.M., 1937. Central part of Chatkal Range. Geology of the Uzbek SSR, vol. 1. ONTI Publishing House, Moscow-Leningrad, pp. 203–254 (in Russian).
Shubin, V.M., Konyukhov, A.A., Bekker, A.Yu., Zakhozhaya, I.G., Faizulin, V.F. et al., 1992. Technical report "Geologicheskoye stroyenie I polezniye iskopayemie ploshchadi listov K-42-60-B; к-42-71-Б; K-42-71-B; K-42-72-A. Otchet Karaburinskoi partii o resultatakh geologicheskoi s'emki masshtaba 1:50 000 na ploshchadi listov K-42-72-A-a, б; K-42-60-B". Bishkek. Geological library of the State Agency for Geology and Mineral Resources (unpublished, in Russian).
Stacey, J.S., Kramers, J.D., 1975. Approximation of terrestrial lead isotopic evolution by two-stage model. Earth Planet. Sci. Lett. 26, 207–221.
Voytenko, V.N., Khudoley, A.K., 2012. Structural evolution of metamorphic rocks in the Talas Alatau, Tien Shan, Central Asia: implication for early stages of the Talas-Ferghana Fault evolution. C.R. Geosci. 344, 138–148. http://dx.doi.org/10.1016/j.crte.2011.11.004.
Wiedenbeck, M., Alle, P., Corfu, F., Griffin, W., Meier, M., Oberli, F., von Quadt, A., Roddick, J.C., Spiegel, W., 1995. Three natural zircon standards for U–Th–Pb, Lu–Hf, trace element and REE analysis. Geostandard Newsl. 19, 1–23.
Williams, I.S., 1998. U-Th-Pb geochronology by ion microprobe. In: McKibben, M.A., Shanks, W.C., III, Ridley, W.I. (Eds.), Applications of Microanalytical Techniques to Understanding Mineralizing Processes, Rev. Econ. Geol., 7, pp. 1–35.
Windley, B.F., Alexeiev, D., Xiao, W., Kröner, A., Badarch, G., 2007. Tectonic models for accretion of the Central Asian Orogenic Belt. J. Geol. Soc. Lond. 164, 31–47.
Yakubchuk, A., Cole, A., Seltmann, R., Shatov, V., 2002. Tectonic setting, characteristics and regional exploration criteria for gold mineralization in central Eurasia: the southern Tien Shan province as a key example. In: Goldfarb, R., Nielsen, R. (Eds.), Integrated Methods for Discovery: Global Exploration in Twenty-First Century. Economic Geology, Special Publication 9, pp. 177–201.
Yakubchuk, A., Schloderer, J., Woodcock, J., Wurst, A., 2010. Taldybulak Au–Cu–Mo deposit: a new >5 Moz Au (11.7 Moz Au eq) Ordovician porphyry hosted gold system in Kyrgyzstan, Central Asia. Appl. Earth Sci. Trans. Inst. Min. Metall. B 119 (2), 84.
Yakubchuk, A., 2017. Evolution of the Central Asia Orogenic Supercollage since late Neoproterozoic revised again. Gondwana Res. http://dx.doi.org/10.1016/j.gr.2016.12.010.
Zonenshain, L.P., Kuzmin, M.I., Natapov, L.M., 1990. Geology of the USSR: A Platetectonic Synthesis, AGU Geodynamics Series 21. American Geophysical Union, Washington, DC, p. 242.
Zubtsov, E.I., Zubtsova, E.I., 1963. Precambrian granites and lower Paleozoic formations of the Middle Tien Shan. DAN USSR 152-4, 945-948 (in Russian).